



## RESEARCH ARTICLE

10.1002/2015EF000315

## Integrating solar energy and climate research into science education

Alan K. Betts<sup>1</sup>, James Hamilton<sup>2</sup>, Sam Ligon<sup>2</sup>, and Ann Marie Mahar<sup>2</sup><sup>1</sup>Atmospheric Research, Pittsford, Vermont, USA, <sup>2</sup>Rutland High School, Rutland, Vermont, USA

## Key Points:

- Data from solar power arrays are a new resource
- Solar flux data are useful for cloud, power, and climate analyses
- Solar data provide local research information for science education

## Corresponding author:

Alan K. Betts, akbetts@aol.com

## Citation:

Betts, A. K., J. Hamilton, S. Ligon, and A. M. Mahar (2016), Integrating solar energy and climate research into science education, *Earth's Future*, 4, 2–13, doi:10.1002/2015EF000315.

Received 6 AUG 2015

Accepted 4 DEC 2015

Accepted article online 6 JAN 2016

Published online 29 JAN 2016

**Abstract** This paper analyzes multi-year records of solar flux and climate data from two solar power sites in Vermont. We show the inter-annual differences of temperature, wind, panel solar flux, electrical power production, and cloud cover. Power production has a linear relation to a dimensionless measure of the transmission of sunlight through the cloud field. The difference between panel and air temperatures reaches 24°C with high solar flux and low wind speed. High panel temperatures that occur in summer with low wind speeds and clear skies can reduce power production by as much as 13%. The intercomparison of two sites 63 km apart shows that while temperature is highly correlated on daily ( $R^2=0.98$ ) and hourly ( $R^2=0.94$ ) timescales, the correlation of panel solar flux drops markedly from daily ( $R^2=0.86$ ) to hourly ( $R^2=0.63$ ) timescales. Minimum temperatures change little with cloud cover, but the diurnal temperature range shows a nearly linear increase with falling cloud cover to 16°C under nearly clear skies, similar to results from the Canadian Prairies. The availability of these new solar and climate datasets allows local student groups, a Rutland High School team here, to explore the coupled relationships between climate, clouds, and renewable power production. As our society makes major changes in our energy infrastructure in response to climate change, it is important that we accelerate the technical education of high school students using real-world data.

## 1. Introduction

Vermont has an ambitious comprehensive energy plan with the goal of meeting 90% of the state's energy needs through renewable resources by 2050 [*Vermont Comprehensive Energy Plan*, 2015]. Part of this is a transition to a distributed renewable energy power system based on solar power and wind farms. In addition, the installed cost of solar power has fallen more than 60% in the past 6 years. As a result, Vermont has seen rapid deployment of solar power projects ranging in scale from small arrays of a few kilowatts (kW) of peak power for individual households, community-shared arrays of a few hundred kilowatts, and much larger megawatt arrays. Since 2011, more than 100 MW of solar photovoltaic (PV) electric generation has been added in the state, and installations proposed for 2016 are increasing in size. At the same time, Green Mountain Power (GMP), the largest electrical utility in Vermont, is moving forward with integrating ever-increasing solar power into a smart grid with distributed electrical storage. On a global scale, non-governmental organizations [e.g., *Solar Electric Light Fund*, 2015] are developing local solar micro-grids that can provide essential power to small communities for lights, communications, irrigation, clinics, and schools, where electrical power from a central grid is unavailable. In coming decades, it is likely that rising sea level, and the rising threat of the collapse of global ecosystems [*Barnosky et al.*, 2012] due to direct human intervention and ongoing climate change driven by a fossil-fuel economy, will drive a rapid global shift to renewables despite powerful resistance from political, economic and financial interests. Vermont has accepted the need for this shift, in part because its own iconic ecosystem is threatened [*ANR*, 2015], and the State has become a leader in the transition towards a renewable energy system. Recently, Rutland Vermont achieved its goal of becoming the city with the most solar power per capita in New England [*Green Mountain Power*, 2015].

This is the context for our analysis of solar power and climate by a Rutland High School team. Solar arrays measure electrical power production, but some arrays also monitor the incoming solar flux and other meteorological parameters, such as temperature and wind speed. These data are transformative as we can now document across the landscape how the solar flux drives maximum temperature and the diurnal range of temperature and infer the role of clouds in reducing the shortwave heating of the surface as well as electrical power production. At the same time, these data, coupled with panel temperature and wind data, elegantly

© 2016 The Authors.

This is an open access article under the terms of the Creative Commons Attribution-NonCommercial-NoDerivs License, which permits use and distribution in any medium, provided the original work is properly cited, the use is non-commercial and no modifications or adaptations are made.

show students the components of the energy balance of a solar-heated surface and give insight into the behavior of the more complex land-surface climate system. The analysis of these datasets provides an excellent opportunity for students to understand the relation between solar flux and power production as well as solar flux and diurnal climate. Both the energy and climate aspects are readily accessible to students, teachers, and the public. The integration of this understanding into the educational system is invaluable because the rapid evolution of the state power infrastructure towards a more sustainable system based on renewable energy requires broad public understanding and support.

The Vermont Experimental Program to Stimulate Competitive Research (VT EPSCoR), under a National Science Foundation grant to the University of Vermont, funds a project called "Research on Adaptation to Climate Change in the Lake Champlain Basin" (RACC). The VT EPSCoR Center for Workforce Development and Diversity (CWDD) at Saint Michael's College, Vermont ([www.uvm.edu/~cwdd](http://www.uvm.edu/~cwdd)) works to integrate students and teachers into the current EPSCoR research with the goal of increasing the diversity of students interested in and pursuing a career in the fields of science, technology, engineering and mathematics. Every year, the CWDD integrates high school teams, consisting of two students, a supervising science teacher and a RACC scientist as mentor, into the RACC research. There were 20 high school teams in 2014–2015 and 18 high school teams in 2015–2016. The application process and the benefits to students and teachers are outlined on the website ([www.uvm.edu/epscor/highschool](http://www.uvm.edu/epscor/highschool)). Every year starts with a week-long residential training session on the Saint Michael's College campus in the summer with an overview of the project, training on data collection and analysis, and instruction on specific projects by a team's mentor. Participants develop skills in scientific methods and Earth systems thinking and experience what it is like to be a scientist. This paper is based on an engineering and climate analysis of data from two solar power sites in Vermont by a Rutland High School team.

From a systems perspective, this project has several essential components. It was designed by the lead author and mentor (AKB) and executed as a merged educational and research project with Rutland High School seniors (JH and SL) and their science teacher (AMM), but it was only possible because of the support of both CWDD and GMP. And beyond this, the state of Vermont has provided extensive policy support for the development of renewable energy sources, especially solar power. The raw data were preprocessed before being given to the students as excel files, together with some suggested analyses. Their science teacher supervised their progress in school on a weekly basis, and their mentor visited the school about monthly to give further advice as their technical and conceptual understanding developed. The students gave an oral presentation of their work at the annual 2015 Vermont EPSCoR student research symposium [for video and PDF, see *Hamilton et al.*, 2015]. Some of this work was also incorporated into their senior capstone projects, for example, the website of *Hamilton* [2015]. The final integration of results into this paper was the responsibility of the lead author.

From a science education perspective, Vermont adopted the Next Generation Science Standards (NGSS) in June 2013. This research project addresses two of the NGSS Performance Expectations (PE) for High Schools [NGSS, 2013]: Engineering Design, specifically HS-ETS1-4, and Earth and Human Activity, specifically HS-ESS3-4. The first, HS-ETS1-4, has the PE "Use a computer simulation to model the impact of proposed solutions to a complex real-world problem with numerous criteria and constraints on interactions within and between systems relevant to the problem." In this case, these 12<sup>th</sup> grade students used spreadsheet analysis to study the complex coupling between solar flux, climate (clouds, temperature and wind), panel temperature, and power generation and address the cross-cutting concept "Systems and system models." The second, HS-ESS3-4, has the PE "Evaluate or refine a technological solution that reduces impacts of human activities on natural systems." In this case, the disciplinary core idea is that "Scientists and engineers can make major contributions by developing technologies that produce less pollution and waste and that preclude ecosystem degradation." Solar arrays are being deployed to reduce CO<sub>2</sub> pollution from the burning of fossil fuels in order to reduce climate change risks. These high school students are analyzing geoscience data to understand the coupling between climate and solar power and some of the operational tradeoffs involved.

This analysis by a Rutland High School team uses data from the GMP solar educational site on Route 7N in Rutland, Vermont for the years 2010–2013 and the comparison with similar data for 2011–2013 from the Ferrisburgh Solar Farm about 63km to the north. After discussing the data processing, we will address both

**Table 1.** Green Mountain Power Rutland Solar Array Variables

Variable	Abbreviation	Units	Instrument
Year			
Day of Year	DOY		
Local Time	LST		
Air Temperature	$T_{\text{air}}$	(°C)	Thermister
Panel Temperature	$T_{\text{panel}}$	(°C)	Thermister
Wind Speed		m/s	Anemometer
Downward Solar Flux	$SW_{\text{dn}}$	$W/m^2$	Li-Cor pyranometer
Panel Solar Flux	$SW_{\text{p}}$	$W/m^2$	Li-Cor pyranometer
Power Generated	Power	kW, kWh/Mo	

climate and engineering questions. We first show the inter-annual differences of temperature, wind, panel solar flux, electrical power production, and cloud cover. Then, we explore the dependence of power generation on the solar flux, which in turn depends on cloud cover and snow covering the panels as well as the impact of solar flux and wind on panel temperature. Then, we explore how the diurnal range of temperature depends on cloud cover. Because distributed solar flux data has become available only recently with the installation of solar arrays, these analyses have a research fascination for students. At the same time, they give important insight into how climate, clouds, and renewable power are part of a coupled system.

Traditionally, measurements of temperature and precipitation have been used to characterize climate because they are routinely available. However, the surface daily solar flux is critically important to the diurnal climate [Betts *et al.*, 2013, 2015]. Historically, only hours of daily sunshine were estimated at climate stations. Now, with the widespread deployment of distributed solar arrays, we are entering a new era for analysis. Some of this analysis was inspired by an exceptional long-term dataset from the Canadian Prairies, which recorded opaque cloud every hour from which the daily solar flux can be calculated [Betts *et al.*, 2013, 2015]. In a broader context, cloud and radiation observations play a critical role in improving our understanding of the climate system. A major uncertainty in our weather forecast and climate models has long been the model computation of the cloud fields [Senior and Mitchell, 1993] and the radiative forcing that depends on them. So these new data from solar arrays, in addition to inspiring a new generation of students, will deepen our observational understanding of the impact of clouds on climate.

## 2. Data Processing

### 2.1. Green Mountain Power Data

Our primary analysis data comes from the Green Mountain Power (GMP) 50 kW solar power educational site on Route 7N in Rutland, Vermont, located at 43° 38' 12''N, 72° 58' 30''W at an elevation of 189m (621ft). We analyze data from 2010–2013. The measured variables include those shown in Table 1.

Figure 1 shows the panel array and the temperature sensor (bottom left) and (bottom right) the pyranometer measuring the solar shortwave flux orthogonal to the panel, abbreviated  $SW_{\text{p}}$  in Table 1. The anemometer measuring wind speed and the pyranometer measuring the downward solar flux on a horizontal surface,  $SW_{\text{dn}}$ , are mounted on the roof of the small brown building behind the solar array. The data were archived as 15-min means. From these, we extracted the daily maximum and minimum air temperatures ( $T_{\text{max}}$  and  $T_{\text{min}}$ ) and derived hourly, daily, and monthly means for all variables. We define the daily or diurnal temperature range as

$$DTR = T_{\text{max}} - T_{\text{min}} \quad (1)$$

### 2.2. Ferrisburgh Solar Farm Data

We have a second dataset from the Ferrisburgh Solar Farm, owned by Pomerleau Real Estate. This is a much larger 1 MW solar array, just south of Ferrisburgh, Vermont, located at 44° 10' 11''N; 73° 14' 25''W at an elevation of 56m (183 ft). This site is 63 km (39 miles) north-north-west of the GMP Rutland site. It has measurements of  $T_{\text{air}}$ ,  $T_{\text{panel}}$ ,  $SW_{\text{p}}$ , and Power generated, archived as 15-min means. We will compare hourly and daily mean  $T_{\text{air}}$  and  $SW_{\text{p}}$  between the two sites for 2011–2013 when we have data from both.



**Figure 1.** Green Mountain Power Solar array (top), air temperature sensor (bottom left), and (bottom right) pyranometer measuring the solar flux orthogonal to the panel.

### 2.3. How Clouds Reduce the Clear-Sky Solar Flux

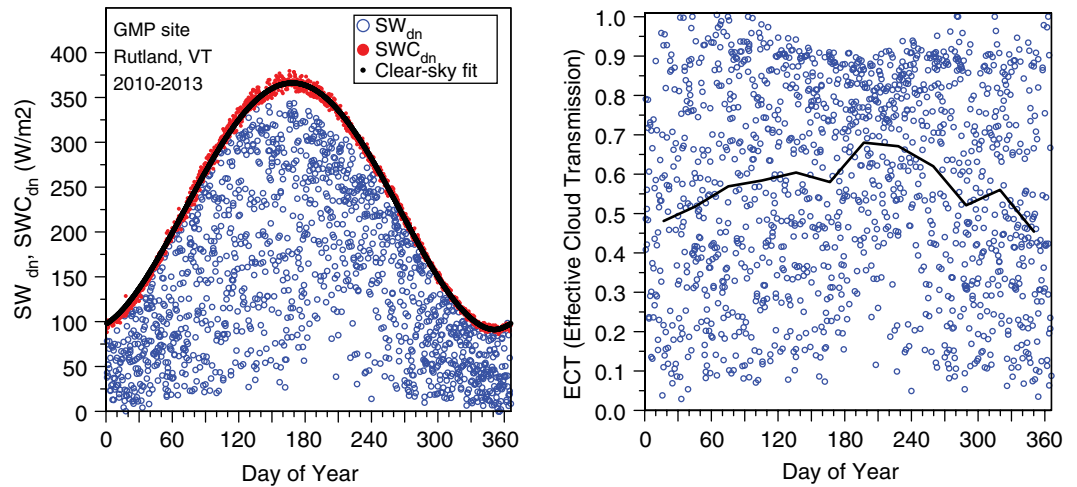
Opaque clouds reflect sunlight, which reduces the downward solar flux below its clear-sky value, so clouds play a crucial role in both climate and electrical power production. It is useful to represent the cloud field by the dimensionless ratio, the Effective Cloud Transmission, defined as

$$ECT = SW_{dn} / SW_{Cdn} \quad (2)$$

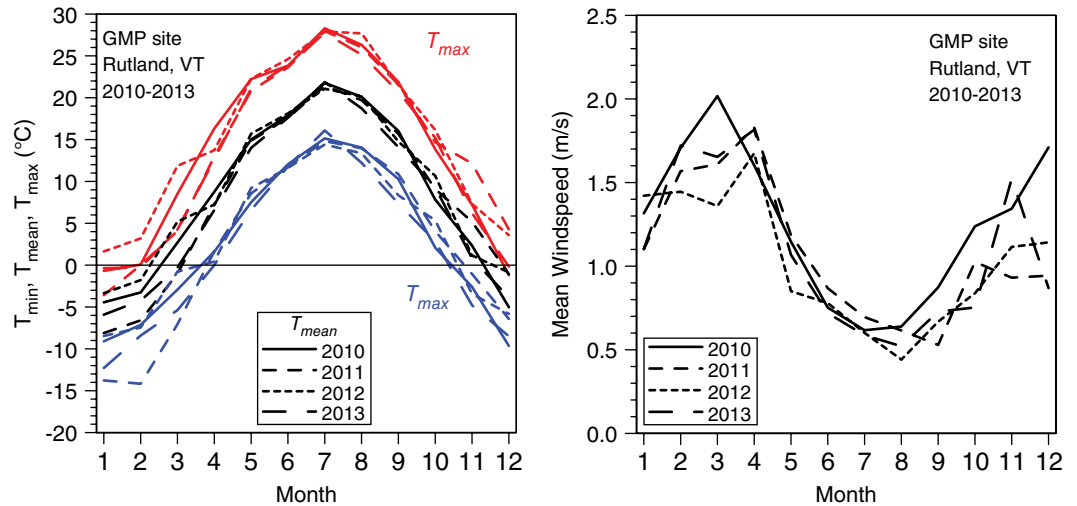
where  $SW_{dn}$  is the measured downward shortwave flux on a horizontal surface, and  $SW_{Cdn}$  is the corresponding clear-sky flux in the absence of clouds. ECT has a range between 0 for very thick overcast skies and 1 for clear skies. *Betts* [2009] defined a corresponding effective cloud albedo as  $ECA = 1 - ECT$ . The clear-sky flux  $SW_{Cdn}$  varies over the year as the elevation of the sun (the solar zenith angle) changes, and we get an estimate on clear-sky days with no clouds. However, it is routinely calculated in models, and here, we use values from the European Weather Centre reanalysis called ERA-Interim [*Dee et al.*, 2011].

Figure 2 illustrates equation (2) using the daily mean measurements of  $SW_{dn}$  for 2010–2013 from the GMP Rutland solar site. The left panel shows measured  $SW_{dn}$  (blue circles) and  $SW_{Cdn}$  (red dots) derived from daily ERA-Interim fluxes (see Appendix) together with a mean fit to the clear-sky data (black line). The clear-sky





**Figure 2.** Measured daily mean downward solar flux and clear-sky solar flux (left) and (right) daily and monthly mean effective cloud transmission.



**Figure 3.** Annual cycle of  $T_{max}$ ,  $T_{mean}$ , and  $T_{min}$  (left) and (right) wind speed for the 4 years.

fluxes form an upper envelope to the  $SW_{dn}$  measurements, with a range from around  $100 \text{ W/m}^2$  at the winter solstice to  $370 \text{ W/m}^2$  at the summer solstice. These values have been averaged over the 24-hr day, including the zeros at night, so they are much less than the peak solar clear-sky flux, which reaches  $1000 \text{ W/m}^2$  near local noon. The reduction of the surface flux by clouds is just the distance between corresponding red and blue points for the same day.

The right panel shows the transformation to the ECT. The day-to-day variability is very large, so we have superimposed the monthly mean values of ECT for 2010–2013 (solid black line). This shows that on average, the cloud field transmits less of the solar energy in winter than in July.

### 3. Monthly Mean Climatology

#### 3.1. Inter-Annual Variability of Temperature and Wind Speed

Rutland Vermont, at a latitude of  $43.637^\circ\text{N}$ , has a large annual cycle of temperature because the solar elevation is higher and day length is longer in summer than in winter. Figure 3 shows the inter-annual differences of temperature and wind speed. On the left, we show the monthly means of maximum temperature,  $T_{max}$  (red), mean air temperature,  $T_{mean}$  (black), and minimum temperature,  $T_{min}$  (blue) for the 4 years. The differences in monthly mean temperature are much larger in winter than in summer because the presence

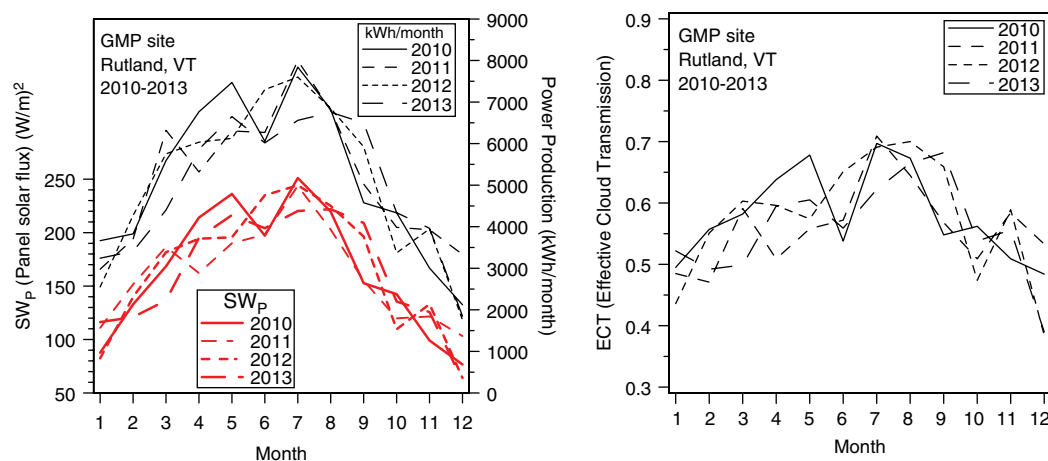


**Figure 4.** Monthly mean solar flux on panels and electrical power production (left) and (right) effective cloud transmission for the 4 years.

or absence of reflective snow cover has a large impact on temperature [Betts, 2011; Betts et al., 2014]. The months January to March 2012, which had little permanent snow cover, were 5°C warmer than the same months in 2011, a winter with more snow. Monthly mean  $T_{max}$  is above freezing in January and February 2012. The right panel shows that the monthly mean wind speeds are lowest in summer, when strong synoptic weather systems are less frequent. The variability in wind speed from year to year is smaller than the range of the annual cycle.

### 3.2. Inter-Annual Variability of Solar Flux, Power Generation, and Cloud Cover

Solar panels convert about 15% of the sun’s energy into electricity, so power production depends on the solar flux normal to the panels,  $SW_p$ , which is measured. Figure 4 (left panel) shows the annual cycle of the measured solar flux and the power production in kWh/month for the 4 years. Both show a minimum in December and a maximum in July, as expected, because the sun is lower in the sky in winter, day-length is shorter, and cloud transmission is less. The year-to-year variation in the monthly mean solar flux and power production are similar because both are reduced by the cloud transmission, shown in the right panel.

## 4. Daily and Hourly Power Production

### 4.1. Daily Power Production

Figure 5 plots the daily mean power production against the daily mean of the solar flux on the panels for the four seasons. The linear regression fit through zero for all the data excluding winter is

$$\text{Power} = 0.0425 (\pm 0.0001) * SW_p \quad (R^2 = 0.997) \quad (3)$$

There is a scattering of points below the line that are mostly in winter. Although we have no snow records at the GMP site, observations from the Rutland Cooperative Observer site confirm that these points below the regression line correspond to days after fresh snowfall. Until it melts, snow cover on the panels reduces power production, and it may also affect the accuracy of the panel solar flux measurement.

### 4.2. Hourly Power Production

Although solar power production depends primarily on the solar energy falling on the panels, the conversion to electricity falls as the panel temperature increases. About 15% of the sun’s energy is converted to electricity, and the rest heats the panels above air temperature, while the ambient wind cools them. In addition, both  $T_{air}$  and wind speed vary seasonally (Figure 3), so these interconnected processes affect power production. Figure 6 (left panels) shows the hourly dependence of array power production on the solar flux, panel temperature, and wind speed. We have selected the 11 hours (0730–1730 LST) roughly centered on

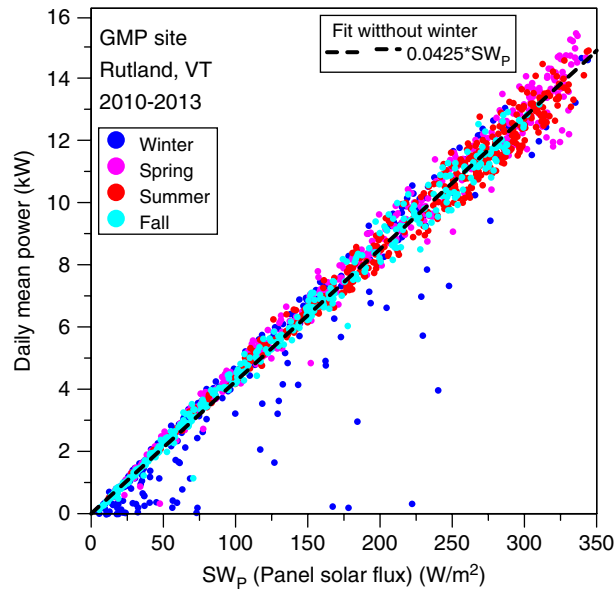


**Figure 5.** Relation between daily mean electrical power and daily mean panel solar flux partitioned by season.

seasonal cycle of temperature and wind. Figure 3 shows that in spring, wind speeds are higher when  $T_{air}$  is lower.

The simple linear regression fit though zero of power on solar flux is the same for the hourly data, as for the daily data shown in Figure 5.

$$\text{Power} = 0.0425 (\pm 0.0000) * SW_p \quad (R^2 = 0.997) \quad (3')$$

If we add the dependence of power on  $T_{panel}$ , scaled by the solar flux, multiple linear regression gives

$$\text{Power} = 0.0478 (\pm 0.0001) * SW_p - 0.143 (\pm 0.002) * (T_{panel} * SW_p / 1000) \quad (R^2 = 0.998) \quad (4)$$

For  $SW_p = 950 \text{ W/m}^2$ , an increase of  $T_{panel}$  by  $40^\circ\text{C}$  reduces power production by 5.4 kW, which is about 13%.

### 4.3. Comparison With Ferrisburgh Solar Farm

Solar arrays are distributed power sources that are integrated by the grid, so it is important to understand the spatial variation across the landscape. The Ferrisburgh Solar Farm is 63 km NNW of the GMP Rutland solar site. Figure 7 compares daily mean  $T_{air}$  and  $SW_p$  for the 3 years 2011–2013. Daily mean temperature is highly correlated between the two sites ( $R^2=0.986$ ). We show the geometric mean of the regression lines of y-on-x and x-on-y. Ferrisburgh, which is 133m (436ft) lower in elevation than the GMP site, is an average  $0.85^\circ\text{C}$  warmer. However, there is uncertainty in this difference because the temperature sensors have not been cross-calibrated.

For the daily mean panel solar flux,  $SW_p$ , and therefore power production, which both depend on cloud cover, the correlation is lower ( $R^2=0.86$ ). We see that the scatter between the two sites is less at the extremes, which represent overcast and nearly clear skies.  $SW_p$  measured at Ferrisburgh is 3.5% higher than at the GMP site. This could represent less cloud cover at Ferrisburgh, but the comparison has some uncertainties. First, the pyranometers have not been cross-calibrated, and their accuracy is only a few percent. Second, the Ferrisburgh panels have a fixed elevation angle, close to  $45^\circ$ , but the elevation of the GMP panels is changed manually by  $10^\circ$  four times a year. The change dates are not precisely recorded (and depend on student availability), but generally, panels are set at  $55^\circ$  October through January, at  $35^\circ$  May through August, and  $45^\circ$  over the spring and fall equinoxes.

local noon and the months April to September. The data has been averaged in  $100 \text{ W/m}^2$  bins,  $10^\circ\text{C}$  bins for panel temperature (top), and  $1 \text{ m/s}$  wind speed bins (bottom). We see that under full sun, mean power production falls with high panel temperature and low wind speed by about 5kW. The right panels show how  $T_{panel}$  and its excess temperature  $\Delta T = (T_{panel} - T_{air})$  depend on solar flux and wind speed. The bottom right panel shows the simple and elegant relation between panel  $\Delta T$ , solar flux, and wind speed.  $\Delta T$  reaches  $24^\circ\text{C}$  at high solar flux and low wind speed. We see that  $\Delta T$  increases as the panels are heated by increasing solar flux and decreases as they are cooled by increasing wind speed. Long-wave radiative cooling of the panels also becomes a significant factor when  $\Delta T$  is large (not shown). The actual panel temperature (upper right),  $(T_{air} + \Delta T)$ , includes the additional complexity of the

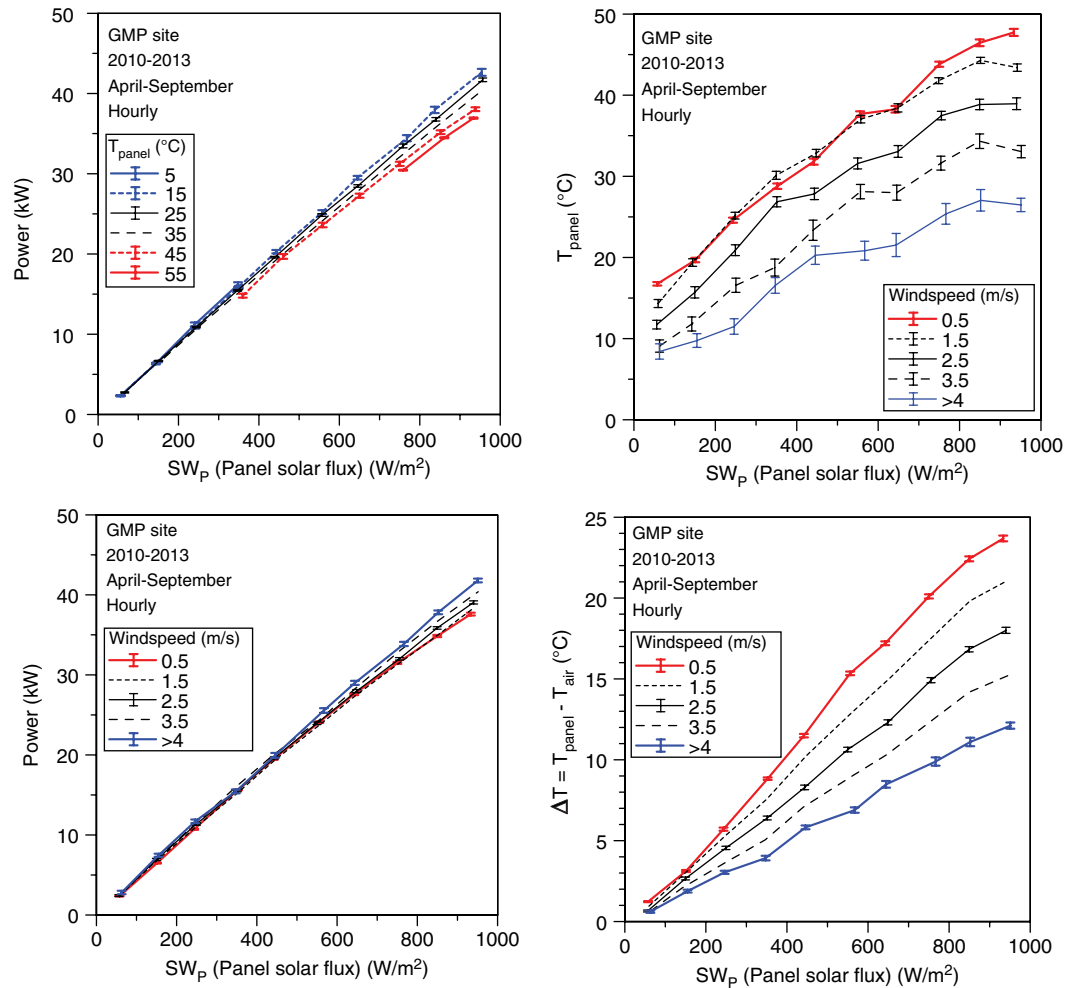


**Figure 6.** Relationships between panel solar flux, power production, panel temperature, and wind speed.

Figure 8 is a similar hourly intercomparison for the months April to September for the seven hourly means between 0930 and 1530 LST. The scatter in hourly temperature is a little larger ( $R^2=0.94$ ) than for the daily means, with a few outliers that could be caused by local rainfall events. Ferrisburgh is a little warmer by  $0.6^\circ\text{C}$  for this near-noon data. The hourly  $SW_p$  comparison shows much more scatter at intermediate values (200–700  $\text{W}/\text{m}^2$ ), representative of broken cloud cover, than at low and high values representative of overcast or nearly clear-sky conditions. For reference, we show the one-to-one line (long dashes) as well as the geometric mean linear regression fit (short dashes). For these hourly data, the mean values for  $SW_p$ :Ferrisburgh and  $SW_p$ :GMP are 601 and 553  $\text{W}/\text{m}^2$ , respectively. This is likely due to some combination of reduced cloud cover at Ferrisburgh and some bias between the shortwave sensors. Under very clear skies in June, with  $SW_p > 950 \text{W}/\text{m}^2$ ,  $SW_p$  is 4% higher at Ferrisburgh than at the GMP site despite the panel elevation being  $35^\circ$  at GMP and  $45^\circ$  at Ferrisburgh.

From a more general perspective, this poor hourly correlation under broken cloud conditions between solar power arrays at 60 km spacing is acceptable, even beneficial, because the power grid can integrate and smooth the cloud-related variability of power production from distributed solar arrays.

### 5. Solar Energy, Clouds, and the Daily Climate

The mean daily cycle of temperature is driven by radiation. At night, the earth's surface cools to space by long-wave radiation, reaching a minimum temperature,  $T_{\text{min}}$ , typically at sunrise. The daytime solar flux heats the surface, and the maximum temperature,  $T_{\text{max}}$ , is typically reached in the early afternoon.



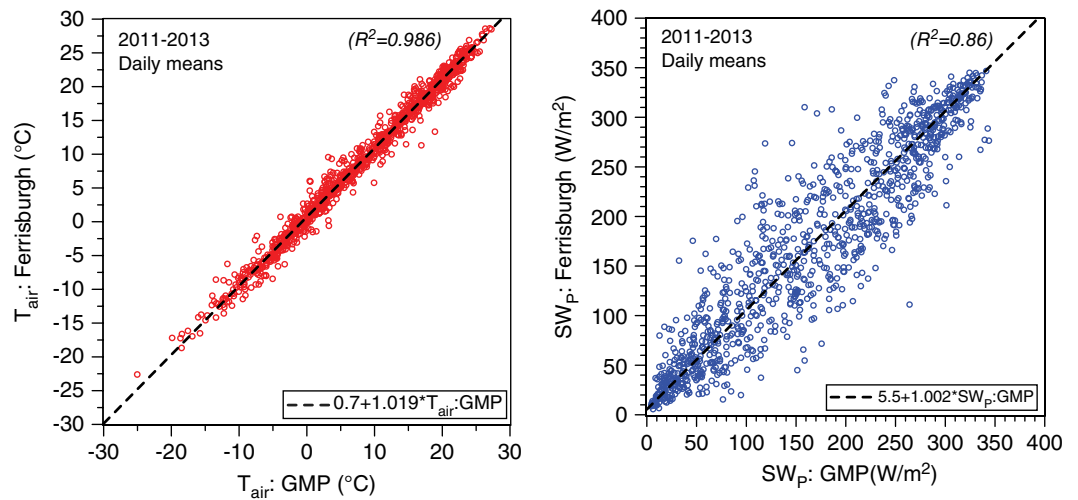


**Figure 7.** Comparison of daily mean  $T_{air}$  (left) and (right)  $SW_p$  between GMP and Ferrisburgh sites. Linear regression fits are shown.

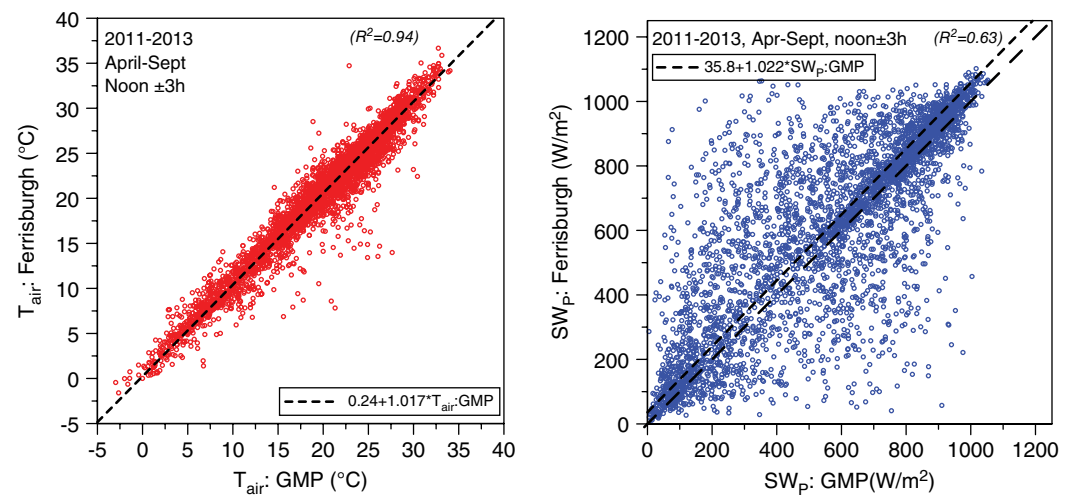


**Figure 8.** Comparison of hourly mean  $T_{air}$  (left) and (right)  $SW_p$  between GMP and Ferrisburgh sites with linear regression fits and (right) one-to-one line.

$DTR = T_{max} - T_{min}$  is the daily or diurnal temperature range (Equation (1)). *Betts et al.* [2013, 2015] showed that in the warmer season months, DTR has a strong dependence on ECT, the fraction of the solar flux transmitted by the cloud field. Snow cover reflects sunlight and reduces the diurnal cycle. In fact, DTR in winter is dominated by synoptic temperature advection, and a winter analysis requires the averaging of more data than we have here [Wang and Zeng, 2014], so we will exclude the winter months.

Figure 9 (left panel) shows the scatterplot of daily DTR against ECT for the months March to November. An upward trend is visible, but there is a lot of day-to-day variation because daily advection of different air masses can impact  $T_{max}$  and  $T_{min}$ . However, if we bin the data in 0.1 ranges of ECT, we get a linear increase of mean DTR with ECT, which has little seasonal dependence (not shown). Under nearly clear skies, mean DTR reaches 16°C. The standard error bars shown are small because there are about 100 days in most bins. The dashed line is the linear regression fit to the binned data with  $R^2 = 0.99$ .

Figure 9 (right panel) compares  $T_{max}$ ,  $T_{min}$  (left scale) and DTR (right scale) from these GMP data with a longer dataset from a Baseline Surface Radiation Network (BSRN) station, 25 km south of Regina, Saskatchewan [Betts et al., 2015]. This BSRN station on the Canadian Prairies is further north at 50.2°N, 104.7°W, where the period with snow cover is longer, so we include only the months April to October. This Canadian Prairie site is primarily flat agricultural land, while the GMP site is on the edge of urban Rutland in a mixed Vermont

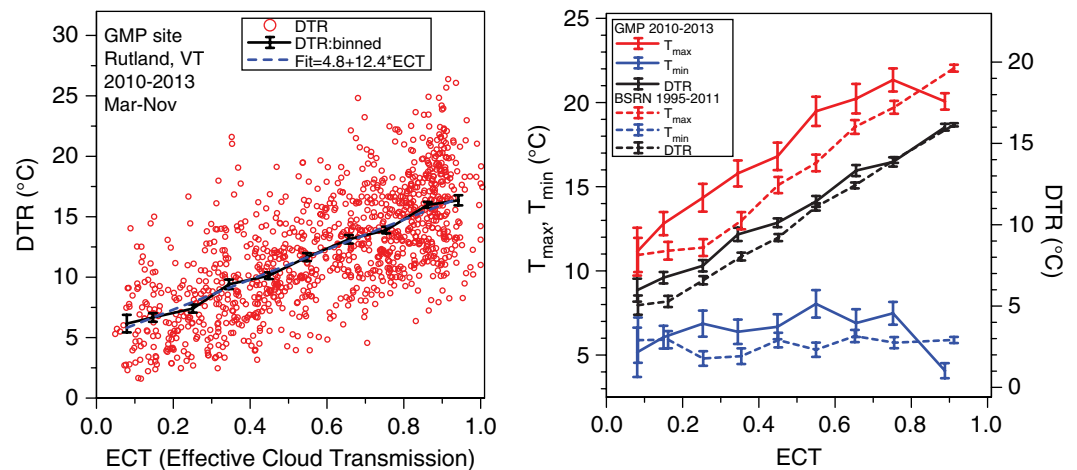


**Figure 9.** Relation between ECT and DTR (left: daily data) and (right) comparison between  $T_{max}$ ,  $T_{min}$  and DTR at GMP site with BSRN site near Regina, Saskatchewan.

landscape of agricultural land and forested hills and mountains. Mean wind speeds are also higher (3.5 m/s) on the Canadian Prairies than at the GMP site. However, the broad trends of the coupling between ECT and daily temperature are similar.  $T_{max}$  and DTR increase with increased solar forcing represented by ECT, while  $T_{min}$  varies rather little. The sharp drop of  $T_{min}$  under clear skies for the GMP site, when night-time cooling is the strongest, might be a local effect of the close proximity of the GMP site to the Green Mountain range. Pico Peak at 1,112m (3647ft) is only 11 km to the east. Using 600 years of Prairie station data, *Betts et al.* [2015] show the effect of wind, relative humidity, and precipitation anomalies on this coupling between DTR and ECT. However, we cannot replicate their analysis with our limited 4-year data set from the GMP site.

### 6. Conclusion

This paper addresses the relationship between the solar flux, clouds, climate, and solar power generation using readily accessible data that can be analyzed by high school students with expert guidance. Analysis of solar flux data, power production, and climate data gives students skills in real-world data analysis, and at the same time, an understanding of how clouds, climate, and renewable energy production are linked together.

We analyzed 4 years of data (2010–2013) from the Green Mountain Power educational site on the north side of Rutland Vermont and 3 years of data (2011–2013) from the Ferrisburgh Solar Farm. First, we quantified the impact of clouds on the surface solar flux as a scaled ECT using corrected clear-sky fluxes from the European Weather Centre reanalysis. We then mapped the monthly climatology of temperature, wind speed, cloud transmission, solar flux, and power production for the GMP site. We derived a linear fit between daily power production and daily panel solar flux, excluding winter when occasional snowfall reduces power production. We then shifted to the hourly timescale and explored the interrelation of power production, panel solar flux, panel temperature, and wind speed. We observed that electrical power drops by 13% at high panel temperatures under low wind speeds.

The comparison of air temperature and panel solar flux between the GMP site and the Ferrisburgh Solar Farm, which are 63 km apart, shows that daily and hourly temperature are well correlated. The correlation of daily mean solar flux between the two sites is also quite good ( $R^2 = 0.86$ ). However, on hourly timescales, panel solar flux is, not surprisingly, less well correlated ( $R^2 = 0.63$ ), particularly when there are broken cloud fields. Given this poor correlation, however, the power grid can integrate and smooth the power production from distributed solar arrays across Vermont.

Finally, we showed the relation between effective cloud transmission of the solar flux and the daily climate represented by the maximum and minimum temperatures and the diurnal range of temperature. The nearly linear increase of DTR and  $T_{max}$  with ECT seen at the GMP site is similar to the relation seen in Canadian Prairie

data. As more solar flux and climate data become available, further analyses will become possible. Because these new solar flux data give insight into the coupling of clouds and climate as well as renewable power production, we strongly recommend that these data be placed in open-access public archives in Vermont and elsewhere for future analysis.

More broadly, this type of research has important social and educational implications. Involving students in research into solar power and climate

1. provides tangible experience of scientific methods and analysis; and
2. spreads understanding of the links between clouds, climate, renewable power, and the societal energy choices that will impact the future of the Earth system.

There has been much discussion about how the public makes sense of and participates in societal decisions about science and technology [e.g., *Nisbet and Scheufele*, 2009]. This project has a specific Vermont context, where the state, professional and citizens groups, and the utilities are actively planning for a sustainable future. Our belief is that as our society makes major changes in our energy infrastructure in response to climate change, we need to accelerate the technical education of high school students using real-world data. The development of Earth-centered systems thinking in society is essential if we are to transform our power system, better manage our waste streams, and move towards a sustainable society [*Betts and Gibson*, 2012].

## Appendix A: Adjustment of the ERA-Interim Clear-Sky Fluxes

The ERA-Interim (abbreviated ERI) clear-sky fluxes are calculated from clear-sky temperature and water vapor profiles and a climatological estimate of atmospheric aerosols. So, they show day-to-day variability, but in a detailed comparison with Baseline Surface Radiation Network (BSRN) station data under clear skies, *Betts et al.* [2015] found that  $SW_{dn}:ERI$  had a low mean bias of order  $-10W/m^2$ . Comparing with the daily mean  $SW_{dn}$  from the GMP data here, which unlike the BSRN data is not calibrated back to international standards, we found a similar low bias under clear skies, so we derived a correction as follows. Adapting the methodology of *Betts et al.* [2015], we fitted a mean annual cycle to the daily mean  $SW_{dn}:ERI$  data

$$SWCFit : ERI = 84 + 268 * (SIN(\pi * DS/365))^{1.8} \quad (A1)$$

where  $DS = DOY + 14$  for  $DOY < 351$ , and  $DOY - 351$  for  $DOY > 350$ , and  $DOY$  stands for Day of Year. We did not make the tiny adjustment for the leap year. This fit to the ERI data has a mean annual bias of  $0.1 \pm 6.2 W/m^2$ , with monthly mean biases that are  $\leq 5 W/m^2$ . However, there are days when measured  $SW_{dn}$  is greater than both  $SW_{dn}:ERI$  and  $SWCFit:ERI$ , so we added a correction with the same  $DOY$  dependence as (A1) to give

$$SWC_{dn} = SW_{dn} : ERI + 7 + 7 * (SIN(\pi * DS/365))^{1.8} \quad (A2)$$

These are the red dots in Figure 1, and the corresponding clear-sky fit shown is

$$Clear-skyFit = 91 + 275 * (SIN(\pi * DS/365))^{1.8} \quad (A3)$$

### Acknowledgments

We thank Green Mountain Power, especially David Dunn, for the data from their Route 7N educational site in Rutland and Pomerleau Real Estate for the data from their Ferrisburgh Solar Farm. We thank John Bixby for advice and Anton Beljaars from ECMWF for the ERA-Interim data for Rutland. This work has been supported by the VT EPSCoR Center for Workforce Development and Diversity, which is funded by the NSF grant EPS1101317 to the University of Vermont. The datasets are available from the first author.

### References

- ANR (2015), Vermont agency of natural resources: Climate change adaptation. [Available at [http://anr.vermont.gov/about\\_us/special-topics/climate-change/adaptation](http://anr.vermont.gov/about_us/special-topics/climate-change/adaptation)]
- Barnosky, A. D., E. A. Hadly, J. Bascompte, E. L. Berlow, J. H. Brown, et al. (2012), Approaching a state shift in Earth's biosphere, *Nature*, 486, 52–58, doi:10.1038/nature11018.
- Betts, A. K. (2009), Land-surface-atmosphere coupling in observations and models, *J. Adv. Model Earth Syst.*, 1(4), 18, doi:10.3894/JAMES.2009.1.4.
- Betts, A. K. (2011), Seasonal climate transitions in New England, *Weather*, 66, 245–248, doi:10.1002/wea.754.
- Betts, A. K., and E. Gibson (2012), Environmental journalism revisited. Ch. 41, in *Environmental Leadership: A Reference Handbook*, edited by D. R. Gallagher, pp. 382–390, SAGE, 9781412981507.
- Betts, A. K., R. Desjardins, and D. Worth (2013), Cloud radiative forcing of the diurnal cycle climate of the Canadian Prairies, *J. Geophys. Res. Atmos.*, 118, 8935–8953, doi:10.1002/jgrd.50593.
- Betts, A. K., R. Desjardins, D. Worth, S. Wang, and J. Li (2014), Coupling of winter climate transitions to snow and clouds over the Prairies, *J. Geophys. Res. Atmos.*, 119, 1118–1139, doi:10.1002/2013JD021168.
- Betts, A. K., R. Desjardins, A. C. M. Beljaars, and A. Tawfik (2015), Observational study of land-surface-cloud-atmosphere coupling on daily timescales, *Front. Earth Sci.*, 3, 13, doi:10.3389/feart.2015.00013.

- Dee, D. P., et al. (2011), The ERA-Interim reanalysis: configuration and performance of the data assimilation system, *Quart. J. Roy. Meteorol. Soc.*, *137*, 553–597.
- Green Mountain Power (2015), The solar capital of New England. [Available at [http://www.greenmountainpower.com/innovative/solar\\_capital/the-solar-capital-of-new-england/](http://www.greenmountainpower.com/innovative/solar_capital/the-solar-capital-of-new-england/)].
- Hamilton, J. (2015), Solar potential in Rutland. <http://jhamiltoncapstone.weebly.com/>
- Hamilton, J., S. Ligon and A. M. Mahar (2015), How does Vermont's climate cater to solar energy? [Available at <http://epscor.w3.uvm.edu/2/node/2634>].
- NGSS (2013), The next generation science standards. [Available at <http://www.nextgenscience.org/next-generation-science-standards>].
- Nisbet, M. C., and C. A. Scheufele (2009), What's next for science communication? Promising directions and lingering distractions, *Am. J. Bot.*, *96*, 1767–1778.
- Solar Electric Light Fund (2015), Energy is a human right. [Available at <http://self.org/>].
- Senior, C. A., and J. F. B. Mitchell (1993), Carbon dioxide and climate: the impact of cloud parameterization, *J. Clim.*, *6*, 393–418.
- Vermont Comprehensive Energy Plan. (2015), 2015 Comprehensive Energy Plan. [Available at [http://publicservice.vermont.gov/publications/energy\\_plan/2015\\_plan](http://publicservice.vermont.gov/publications/energy_plan/2015_plan)].
- Wang, A., and X. Zeng (2014), Range of monthly mean hourly land surface air temperature diurnal cycle over high northern latitudes, *J. Geophys. Res. Atmos.*, *119*, 5836–5844, doi:10.1002/2014JD021602.